



Sparsity-aware DOA estimation of quasi-stationary signals using nested arrays



Yuexian Wang^{a,*}, Ahmad Hashemi-Sakhtsari^b, Matthew Trinkle^a, Brian W.-H. Ng^a

^a University of Adelaide Radar Research Centre, School of Electrical and Electronic Engineering, The University of Adelaide, Adelaide, SA 5005, Australia

^b National Security and Intelligence, Surveillance and Reconnaissance Division, Defence Science and Technology Group, Edinburgh, SA 5111, Australia

ARTICLE INFO

Article history:

Received 24 April 2017

Revised 22 August 2017

Accepted 29 September 2017

Available online 29 September 2017

Keywords:

Direction of arrival (DOA)

Quasi-stationary signals (QSS)

Nested array

Sparse reconstruction

ABSTRACT

Direction of arrival (DOA) estimation of quasi-stationary signals (QSS) impinging on a nested array in the context of sparse representation is addressed in this paper. By exploiting the quasi-stationarity and extended virtual array structure provided inherently in the nested array, a new narrowband signal model can be obtained, achieving more degrees of freedom (DOFs) than the existing solutions. A sparsity-based recovery algorithm is proposed to fully utilise these DOFs. The suggested method is based on the sparse reconstruction for multiple measurement vector (MMV) which results from the signal subspace of the new signal model. Specifically, the notable advantages of the developed approach can be attributed to the following aspects. First, through a linear transformation, the redundant components in the signal subspace can be eliminated effectively and a covariance matrix with a reduced dimension is constructed, which saves the computational load in sparse signal reconstruction. Second, to further enhance the sparsity and fit the sampled and the actual signal subspace better, we formulate a sparse reconstruction problem that includes a reweighted ℓ_1 -norm minimisation subject to a weighted error-constrained Frobenius norm. Meanwhile, an explicit upper bound for error-suppression is provided for robust signal recovery. Additionally, the proposed sparsity-aware DOA estimation technique is extended to the wideband signal scenario by performing a group sparse recovery across multiple frequency bins. Last, upper bounds of the resolvable signals are derived for multiple array geometries. Extensive simulation results demonstrate the validity and efficiency of the proposed method in terms of DOA estimation accuracy and resolution over the existing techniques.

© 2017 Elsevier B.V. All rights reserved.

1. Introduction

Direction of arrival (DOA) estimation, which determines the spatial spectra of the impinging electromagnetic or acoustic waves by using sensor arrays, has been attracting considerable attention due to its application to various fields, for instance radar, sonar, and microphone array systems, to name a few. It is well known that an M -element uniform linear array (ULA) has $M - 1$ degrees of freedom (DOFs), i.e., it can resolve up to $M - 1$ sources or targets by using conventional subspace-based DOA estimation methods, such as MUSIC [1] and ESPRIT [2]. On the other hand, a higher number of DOFs can be achieved to identify more sources by using either distinct characteristics embedded in the signals, like noncircularity [3] of wireless communication signals and orthogonality

between transmitted signals in MIMO radar [4], or the same number of sensors but sparsely placed [5,6].

Quasi-stationary signals (QSS) represent an important class of signals that we frequently encounter in many applications such as microphone array speech processing [7] and electroencephalogram [8]. The QSS have the statistical property that remains locally static over a short period of time but varies from one local time frame to another. DOA estimation of such audio or speech signals plays an important role, for example, in teleconference systems and automatic conference minute generators. Such real-world applications usually are challenged by scenarios where more sources than the number of sensors are present simultaneously, which turns out to the so-called underdetermined DOA estimation problem. Recently, a Khatri-Rao (KR) subspace approach has been proposed in [9] to tackle this kind of issue for QSS. The work in [9] reveals that the quasi-stationarity in the time domain is not only favourable to the enhancement of DOFs in the spatial domain, i.e., $2(M - 1)$ sources can be estimated with M physical sensors, but is also robust to unknown coloured noise. This work is then extended to

* Corresponding author.

E-mail addresses: jwang@eleceng.adelaide.edu.au (Y. Wang), ahmad.hashemi-sakhtsari@dsto.defence.gov.au (A. Hashemi-Sakhtsari), mtrinkle@eleceng.adelaide.edu.au (M. Trinkle), brian.ng@adelaide.edu.au (B.W.-H. Ng).

two-dimensional array geometry, i.e., uniform circular array (UCA), and corresponding DOFs that the subspace method is able to provide is studied in [10].

To increase the number of resolvable sources beyond the number of given physical sensors, an alternative is to leverage sparse array geometries, such as emerging nested arrays [11], which are capable of providing $\mathcal{O}(M^2)$ DOFs with $\mathcal{O}(M)$ physical sensors. The idea behind this systematic sparse array design lies in achieving the higher number of DOFs by exploiting the difference co-array whose virtual sensor positions are determined by the lag differences between the physical sensors. The nested array is considered attractive as its synthetic geometry is equivalent to a ULA with larger apertures and DOFs which have a closed form expression with respect to the given number of sensors. Inspired by [11], much effort has been devoted to DOA estimation using nested arrays. In particular, by exploiting a four-level nested array with M elements, the subspace-based method in [12] further increases the identifiability to $\mathcal{O}(M^4)$ QSS.

Since the observations from the virtual array are obtained through vectorising the covariance matrix of the nested array, which is equivalent to signals with one snapshot impinging on the synthetic array, it intuitively entails a strong motivation for utilising rank restoration techniques, including spatial smoothing [11] and matrix restoration [13], to enable subsequent subspace-based methods to work properly. In [14], a hybrid approach is presented that uses a low-rank matrix denoising algorithm followed by a MUSIC-like method for DOA estimation.

In recent years, a novel approach, referred to as sparse signal reconstruction, has been introduced for statistical signal analysis and parameter estimation, exhibiting remarkable superiority in resolution and robustness to noise. Distinct from the principle of rank restoration, sparse reconstruction determines the DOA estimates by finding the sparsest supports which index an over-complete basis with respect to angular grids, without being confined by the condition of rank which is necessary for the subspace-based methods. The sparse signal reconstruction process can be regarded as the ℓ_0 -norm optimisation problem. Unfortunately, it is nonconvex and NP-hard to solve [15,16].

To overcome this difficulty, many algorithms have been proposed for convex relaxation, e.g., ℓ_p -norm, $0 < p \leq 1$, optimisation. In [17], a recursive weighted least-squares algorithm called FO-CUSS is addressed for achieving sparsity with a single measurement vector (SMV) in the problem of DOA estimation. In [18], the vector formed by the beamformer outputs is considered as a sparse linear combination of bases of beamformer outputs by the global matched filter (GMF). So far, the most representative sparse recovery algorithm for DOA estimation is ℓ_1 -SVD [19], which exploits the ℓ_1 -norm penalty to enforce sparsity in conjunction with singular value decomposition (SVD) for dimension reduction of the problem size. A merit of the ℓ_1 -SVD is that it is applicable to not only the SMV case but also the multiple measurement vector (MMV) problem. Although the ℓ_1 -norm minimisation is a convex problem and the global minima can be guaranteed easily, it has inherent drawbacks: one is the equal penalisation which is actually prejudiced for large supports, and the other is suboptimal regularisation between the sparsity penalty and subspace fitting error, sometimes resulting in unsatisfactory sparse recovery especially at low signal-to-noise ratio (SNR).

To alleviate this problem, the iterative reweighted ℓ_1 minimisation [20] was developed, where large weights are used to punish the entries who are more likely to be zero in recovered signals, whereas small weights are used to preserve the large entries. Based on [19,20], Xu et al. proposed the weighted ℓ_1 -norm penalty utilising the property of the Capon spectrum function, referred to as CSW- ℓ_1 , to improve the performance of ℓ_1 -norm minimisation, and a theoretical guidance of selecting the regularisation

parameter has been offered in their work [21]. Sparse representation of array covariance vectors (SRACV) [22] also employed the ℓ_1 -norm penalty to reconstruct the covariance vectors, while it addressed the problem in the correlation domain instead of the raw data domain. Following the work of [22], Hu et al. attempted to obtain the DOA estimates by solving an ℓ_2 -norm minimisation subject to a constrained ℓ_1 -norm [23], but the upper bound of the sparse vector is experimentally determined and no theoretically guaranteed quantity is provided. The sparse spectrum fitting (SpSF) algorithm [24] has well elaborated on the best choice of regularisation parameter for DOA and power estimation, with a reduced computational complexity. More recently, similar work has been followed by Tian et al., and a sparse representation of second-order statistics vector and ℓ_0 -norm approximation (SRSSV- ℓ_0) [25] has been discussed. In the work, a surrogate truncated ℓ_1 function was exploited to approximate the ℓ_0 -norm, and the nonconvex minimisation problem can be handled by the difference of convex functions decomposition. Without choosing any hyperparameters such as the methods mentioned above, a sparse iterative covariance-based estimation (SPICE) [26] approach was proposed for array signal processing by the minimisation of a covariance matrix fitting criterion. Instead of approximating the ℓ_0 -norm with the ℓ_1 -norm, Hyder and Mahata exploit a family of Gaussian functions to deal with the ℓ_1 -norm approximation problem, and further propose an alternative strategy named JLZA-DOA [27]. However, as the iteratively updating Gaussian variances are chosen subjectively, global minima is not guaranteed.

As it becomes clear from the aforementioned discussion, the superiority of the nested array and sparse reconstruction motivate us to incorporate them to cope with DOA estimation of QSS, with further enhanced DOFs and even larger effective array aperture. It is essential for QSS to stack the KR products of covariance matrices of local frames, to achieve the array aperture expansion, nevertheless, directly applying some sparsity-inducing algorithms, like SRACV and SRSSV- ℓ_0 , to these KR products, which can be regarded as multiple pseudo snapshots of the expanded virtual array, cannot achieve higher DOFs as these methods are designed for the SMV not the MMV problem in the correlation domain herein. In addition, there is no reason to believe that the pseudo signals, i.e., the covariances of the true signals in each frame, are uncorrelated to each other or the number of pseudo snapshots (frames) is sufficiently large to ensure the uncorrelation, so a transformation of the MMV to the virtual SMV problem in the sparse signal representation framework, as [22,25] have done, is not applicable. On the other hand, though other sparse recovery methods, e.g., ℓ_1 -SVD, CSW- ℓ_1 , and SpSF, can deal with the MMV problem, they require *a priori* knowledge of noise statistics to determine the regularisation parameter, but this is not available in the model of pseudo snapshots generated from QSS. Consequently, by utilising a nested array in conjunction with the sparse representation framework in the case of QSS, new strategies for solving the correlation-aware support recovery problem with MMV are desired.

In this paper, the DOA estimation of QSS is performed by employing a novel sparse weighted subspace reconstruction (SWSR) with a nested array. We first introduce the sparse representation framework for MMV to the QSS case, and provide a reasonable selection of the weights for the ℓ_1 -norm penalty, to further enforce the sparsity and approximate the original ℓ_0 -norm, and the regularisation parameter for the subspace fitting error, to guarantee robust sparse recovery. Besides, we derive the analytical expression of the available number of DOFs as a function of the number of physical sensors, M , and show that the maximum identifiability of the proposed method is $\mathcal{O}(M^2)$ which is twice as many as for ordinary nested array processing as the additional quasi-stationarity is exploited herein. Second, the proposed sparsity-aware scheme is extended to the wideband signal case using $\ell_{2,1}$ -norm sparse

regularisation. The wideband extension of the narrowband algorithm is not a simple average of the results obtained from different frequency bins, and a new formulation based on the group sparsity concept has to be applied to effectively exploit the information carried across the frequency bands of wideband signals, resulting in suppression of the spatial aliasing. As we shall show in the subsequent sections, the proposed method has a better estimation accuracy, a larger identifiability, and a superior resolution compared with the existing techniques. Analytical and numerical simulation results will both be given to support each other in the ensuing development.

It should be noted that a similar research issue has been addressed in [28], where the fourth-order difference co-array is exploited to gain higher DOFs. The main distinctions between SWSR and the method in [28], SAFE-CPA, are stark, which lie in: (a) SAFE-CPA virtually expands the physical array to have a much larger aperture, implemented by vectorising covariance matrices twice¹, which highly relies on the assumption that the powers of QSS are wide-sense stationary and uncorrelated with each other. However, the prerequisite cannot always satisfy real applications when the signal powers are correlated to each other, or signal quasi-stationarity cannot last for long, say several dozens of frames, which will also incur the partially correlated power case that is particularly relevant in the frame-starved scenario. In contrast, SWSR accommodates correlation between source powers even if they are fully correlated; (b) SAFE-CPA converts DOA estimation into solving a basis pursuit denoising problem, and the key parameter therein, error bound preserving the data fidelity, is chosen through trial-and-error in every experiment, which involves extra computations and is not pragmatic in real applications, whereas SWSR not only explicitly provides such an upper bound in a mathematical expression that can guarantee the signal subspace fidelity will be satisfied with a high probability, but also enforce weights on sparse supports to make ℓ_1 norm further approximate ℓ_0 norm; (c) SAFE-CPA is designed for quasi-stationary signals contaminated by white Gaussian noise, whereas SWSR is robust to spatially coloured noise. These differences enable SWSR to have its own advantages on DOA estimation of QSS.

The rest of the paper is organised as follows. The DOA estimation model of QSS in a nested array is introduced in Section 2. The proposed sparsity-aware algorithm is discussed in detail first based on the narrowband signal condition then extended to the wideband scenario in Section 3, where some mathematical analysis relating to the maximum number of resolvable signals is also performed. Section 4 provides extensive numerical simulations demonstrating the advantages of our method in terms of DOFs, estimation resolution, and accuracy. Finally, some concluding remarks are drawn in Section 5.

Notations: We use lower-case (upper-case) bold characters to denote vectors (matrices). In particular, the operators $(\cdot)^T$, $(\cdot)^*$, $(\cdot)^H$, $(\cdot)^{-1}$, $E[\cdot]$, \otimes , and \circ denote the operation of transpose, conjugate, conjugate transpose, inverse, expectation, Kronecker product, and Khatri-Rao product, respectively. The complex operator j is reserved for the imaginary unit, i.e., $j = \sqrt{-1}$. The notations $\Pr\{\cdot\}$, $\text{rank}(\cdot)$, and $\text{vec}(\cdot)$ denote the probability of an event, rank of a matrix, and the vectorisation operator that turns a matrix into a vector by stacking all columns on top of each other, respectively. $\|\cdot\|_0$, $\|\cdot\|_1$, $\|\cdot\|_2$, and $\|\cdot\|_F$ denote the ℓ_0 , ℓ_1 , Euclidean (ℓ_2), and Frobenius norms, respectively. The symbol $\text{diag}\{z_1, z_2\}$ represents a diagonal matrix with diagonal entries z_1, z_2 and $\text{blkdiag}\{\mathbf{Z}_1, \mathbf{Z}_2\}$ represents a block diagonal matrix with diagonal entries $\mathbf{Z}_1, \mathbf{Z}_2$. The symbol $\mathbf{Z}(a:b, c:d)$ denotes a constructed submatrix with the en-

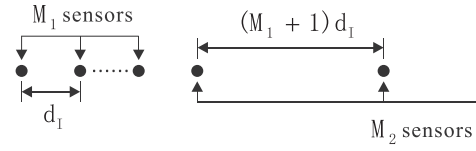


Fig. 1. Schematic of a 2-level nested array with M_1 sensors in the inner ULA and M_2 sensors in the outer ULA.

tries from the a to b th row and c to d th column of \mathbf{Z} , and the symbol $\mathbf{Z}(a, b)$ denotes the entry in the a th row and b th column of \mathbf{Z} .

2. Problem formulation

We assume there is a nonuniform linear nested array with M sensors, consisting of two concatenated ULAs. Suppose the inner ULA has M_1 sensors with inter-element spacing d_1 and the outer ULA has M_2 sensors with inter-element spacing $d_0 = (M_1 + 1)d_1$. The inter-element spacing d_1 is typically set to $\frac{\lambda}{2}$, where λ denotes the wavelength. More precisely, a 2-level nested array, as shown in Fig. 1, is a linear array with sensor locations given by the union of the sets S_I and S_O ,

$$\begin{aligned} P &= S_I \cup S_O \\ &= \{md_1 | m = 0, \dots, M_1 - 1\} \\ &\quad \cup \{(n(M_1 + 1) + M_1)d_1 | n = 0, \dots, M_2 - 1\} \end{aligned} \quad (1)$$

Note that if the i th element of P is denoted as p_i , then $p_1 = 0$, i.e., the first sensor is assumed as the reference. Consider a number of N narrowband far-field signals impinging on the array. The corresponding $M \times 1$ array observation vector is then given by

$$\mathbf{x}(t) = \sum_{i=1}^N \mathbf{a}(\theta_i) s_i(t) + \mathbf{n}(t) = \mathbf{A}\mathbf{s}(t) + \mathbf{n}(t) \quad (2)$$

where $\mathbf{a}(\theta_i) = [1, e^{j\frac{2\pi p_2}{\lambda} \sin \theta_i}, \dots, e^{j\frac{2\pi p_M}{\lambda} \sin \theta_i}]^T \in \mathbb{C}^M$ is the steering vector, $\mathbf{A} = [\mathbf{a}(\theta_1), \dots, \mathbf{a}(\theta_N)]$ is the array manifold, and $\mathbf{s}(t) = [s_1(t), \dots, s_N(t)]^T$. We assume that the source signals $\{s_i(t)\}_{i=1}^N$ are uncorrelated to each other and have zero-mean, the noise vector $\mathbf{n}(t)$ is zero-mean wide-sense stationary (WSS) with an unknown covariance matrix \mathbf{R}_n , and it is uncorrelated to the signals. Besides, we assume that \mathbf{A} is unambiguous, i.e., the steering vectors $\{\mathbf{a}(\theta_i)\}_{i=1}^N$ are linearly independent for any set of distinct $\{\theta_i\}_{i=1}^N$.

In this paper, the signals $\{s_i(t)\}_{i=1}^N$ are modeled as quasi-stationary processes with K non-overlapped frames and the length of each frame is L . Within the k th frame, the QSS are stationary, i.e.,

$$E\{|s_i(t)|^2\} = \sigma_{ik}^2, \quad \forall t \in [(k-1)L, kL-1], \quad k = 1, 2, \dots, K \quad (3)$$

where the signal power σ_{ik}^2 varies with i and k . The corresponding exact local covariance in the k th frame can be expressed as

$$\mathbf{R}_k = E[\mathbf{x}_k(t)\mathbf{x}_k^H(t)] = \mathbf{A}\mathbf{D}_k\mathbf{A}^H + \mathbf{R}_n \quad (4)$$

where $\mathbf{D}_k = \text{diag}\{\sigma_{1k}^2, \dots, \sigma_{Nk}^2\}$, and $\mathbf{x}_k(t)$ contains the snapshots within the k th frame.

Vectorising the covariance matrix \mathbf{R}_k , one has

$$\begin{aligned} \mathbf{y}_k &= \text{vec}(\mathbf{R}_k) = \text{vec}(\mathbf{A}\mathbf{D}_k\mathbf{A}^H) + \text{vec}(\mathbf{R}_n) \\ &= \text{vec}\left(\sum_{i=1}^N \sigma_{ik}^2 \mathbf{a}(\theta_i)\mathbf{a}^H(\theta_i)\right) + \text{vec}(\mathbf{R}_n) \\ &= (\mathbf{A}^* \circ \mathbf{A})\mathbf{q}_k + \text{vec}(\mathbf{R}_n) \end{aligned} \quad (5)$$

where $\mathbf{A}^* \circ \mathbf{A} = [\mathbf{a}^*(\theta_1) \otimes \mathbf{a}(\theta_1), \mathbf{a}^*(\theta_2) \otimes \mathbf{a}(\theta_2), \dots, \mathbf{a}^*(\theta_N) \otimes \mathbf{a}(\theta_N)]$ and $\mathbf{q}_k = [\sigma_{1k}^2, \dots, \sigma_{Nk}^2]^T$. In fact, Eq. (5) follows the property of KR

¹ SAFE-CPA is an array configuration for DOFs improvement. There are several implementations, and extending virtual array structure via vectorising the covariance matrix twice is one way.

product which has been used in the literature, e.g., [9,29], and is equivalent to a new signal model where N signals in \mathbf{q}_k impinge on a linear array giving a single snapshot observation \mathbf{y}_k , and $\mathbf{A}^* \circ \mathbf{A}$ is virtually the array manifold.

3. Sparsity-aware DOA estimation of quasi-stationary signals

3.1. Narrowband signal estimation

We first stack \mathbf{y}_k , $k = 1, \dots, K$, in a row and obtain

$$\mathbf{Y} = [\mathbf{y}_1, \mathbf{y}_2, \dots, \mathbf{y}_K] = (\mathbf{A}^* \circ \mathbf{A}) \mathbf{\Xi} + \text{vec}(\mathbf{R}_n) \mathbf{1}_K^T \quad (6)$$

where $\mathbf{\Xi} = [\mathbf{q}_1, \mathbf{q}_2, \dots, \mathbf{q}_K]$ and $\mathbf{1}_K = [1, 1, \dots, 1]^T \in \mathbb{R}^K$. As the signal power distributions over the time frames are different, $\mathbf{\Xi}$ can maintain full row rank on condition that $K \geq N + 1$. The signals whose power spectrums are not flat can satisfy this condition in the real world, such as most sound or acoustic signals.

To eliminate the unknown noise effect, one can perform an orthogonal projector $\mathbf{P}_{\mathbf{1}_K}^\perp = \mathbf{I}_K - \frac{1}{K} \mathbf{1}_K \mathbf{1}_K^T$ to \mathbf{Y} as

$$\mathbf{Y} \mathbf{P}_{\mathbf{1}_K}^\perp = (\mathbf{A}^* \circ \mathbf{A}) \mathbf{\Xi} \mathbf{P}_{\mathbf{1}_K}^\perp. \quad (7)$$

It can be readily seen that $\mathbf{Y} \mathbf{P}_{\mathbf{1}_K}^\perp$ contains K noise-free observations collected from the virtual array, whose manifold is $\mathbf{A}^* \circ \mathbf{A}$, receiving pseudo signals $\mathbf{\Xi} \mathbf{P}_{\mathbf{1}_K}^\perp \in \mathbb{R}^{N \times K}$. It is obvious to identify that $\text{rank}(\mathbf{\Xi} \mathbf{P}_{\mathbf{1}_K}^\perp) = \text{rank}(\mathbf{\Xi}) = N$, and thus $\text{rank}(\mathbf{Y} \mathbf{P}_{\mathbf{1}_K}^\perp) = N$.

Note that $\mathbf{A}^* \circ \mathbf{A} \in \mathbb{C}^{M^2 \times N}$ has larger DOFs and effective aperture. The increased DOFs directly depend on the distinct rows of $\mathbf{A}^* \circ \mathbf{A}$, which corresponds to the lag $p_m - p_n$ between elements of the location set P . It is known that there are $2M_2(M_1 + 1) - 1$ distinct consecutive lags for the 2-level nested array provided that the signals are uncorrelated [11], so one can exploit this property yielded from the difference co-array to handle the underdetermined DOA estimation problem. Since $2M_2(M_1 + 1) - 1 < M^2$, which implies that there exists redundant rows in $\mathbf{A}^* \circ \mathbf{A}$, one can reduce the problem dimension prior to proceeding to the sparse recovery method.

Considering the nested array as a subset of a ULA with a steering vector $\mathbf{b}(\theta_i) = [1, e^{j\frac{2\pi d_L}{\lambda} \sin \theta_i}, \dots, e^{j\frac{2\pi (M_1 M_2 + M_2 - 1) d_L}{\lambda} \sin \theta_i}]^T \in \mathbb{C}^{M_1 M_2 + M_2}$, there is a relationship between their array manifolds

$$\mathbf{A} = \mathbf{F} \mathbf{B} \quad (8)$$

where $\mathbf{F} = [\mathbf{e}_{\frac{p_1}{d_L} + 1}, \mathbf{e}_{\frac{p_2}{d_L} + 1}, \dots, \mathbf{e}_{\frac{p_M}{d_L} + 1}]^T \in \mathbb{R}^{M \times (M_1 M_2 + M_2)}$ is a selection matrix, $\mathbf{e}_i \in \mathbb{R}^{M_1 M_2 + M_2}$, $i = \frac{p_1}{d_L} + 1, \frac{p_2}{d_L} + 1, \dots, \frac{p_M}{d_L} + 1$, is a column vector with 1 at the i th entry and 0 elsewhere, and $\mathbf{B} = [\mathbf{b}(\theta_1), \dots, \mathbf{b}(\theta_N)]$.

Therefore, one has

$$\begin{aligned} \mathbf{A}^* \circ \mathbf{A} &= (\mathbf{F} \mathbf{B})^* \circ (\mathbf{F} \mathbf{B}) \\ &= [\mathbf{F} \mathbf{b}^*(\theta_1), \dots, \mathbf{F} \mathbf{b}^*(\theta_N)] \circ [\mathbf{F} \mathbf{b}(\theta_1), \dots, \mathbf{F} \mathbf{b}(\theta_N)] \\ &= [(\mathbf{F} \mathbf{b}^*(\theta_1)) \otimes (\mathbf{F} \mathbf{b}(\theta_1)), \dots, (\mathbf{F} \mathbf{b}^*(\theta_N)) \otimes (\mathbf{F} \mathbf{b}(\theta_N))] \\ &= [(\mathbf{F} \otimes \mathbf{F})(\mathbf{b}^*(\theta_1) \otimes \mathbf{b}(\theta_1)), \dots, (\mathbf{F} \otimes \mathbf{F})(\mathbf{b}^*(\theta_N) \otimes \mathbf{b}(\theta_N))] \\ &= (\mathbf{F} \otimes \mathbf{F})(\mathbf{B}^* \circ \mathbf{B}). \end{aligned} \quad (9)$$

Referring to [9], one knows that

$$\mathbf{B}^* \circ \mathbf{B} = \mathbf{G} \tilde{\mathbf{B}} \quad (10)$$

where $\tilde{\mathbf{B}} = [\tilde{\mathbf{b}}(\theta_1), \dots, \tilde{\mathbf{b}}(\theta_N)]$ with $\tilde{\mathbf{b}}(\theta_i) = [e^{j\frac{2\pi (M_1 M_2 + M_2 - 1) d_L}{\lambda} \sin \theta_i}, e^{j\frac{2\pi (M_1 M_2 + M_2 - 2) d_L}{\lambda} \sin \theta_i}, \dots, 1, \dots, e^{-j\frac{2\pi (M_1 M_2 + M_2 - 1) d_L}{\lambda} \sin \theta_i}]^T \in$

$\mathbb{C}^{2(M_1 M_2 + M_2) - 1}$ and

$$\mathbf{G} = \begin{bmatrix} 0 & \dots & 0 & 1 & 0 & \dots & 0 \\ 0 & \dots & 0 & 0 & 1 & \dots & 0 \\ \vdots & \ddots & \vdots & \vdots & \vdots & \ddots & \vdots \\ 0 & \dots & 0 & 0 & 0 & \dots & 1 \\ 0 & \dots & 1 & 0 & 0 & \dots & 0 \\ 0 & \dots & 0 & 1 & 0 & \dots & 0 \\ \vdots & \ddots & \vdots & \vdots & \ddots & \vdots & \vdots \\ 0 & \dots & 0 & 0 & \dots & 1 & 0 \\ \vdots & \vdots & \vdots & \vdots & \vdots & \vdots & \vdots \\ 1 & 0 & \dots & 0 & 0 & \dots & 0 \\ 0 & 1 & \dots & 0 & 0 & \dots & 0 \\ \vdots & \vdots & \ddots & \vdots & \vdots & \ddots & \vdots \\ 0 & 0 & \dots & 1 & 0 & \dots & 0 \end{bmatrix} \in \mathbb{R}^{(M_1 M_2 + M_2)^2 \times (2(M_1 M_2 + M_2) - 1)}. \quad (11)$$

Substituting (10) into (9), one finds that

$$\mathbf{A}^* \circ \mathbf{A} = (\mathbf{F} \otimes \mathbf{F}) \mathbf{G} \tilde{\mathbf{B}}, \quad (12)$$

so

$$\mathbf{Y} \mathbf{P}_{\mathbf{1}_K}^\perp = (\mathbf{F} \otimes \mathbf{F}) \mathbf{G} \tilde{\mathbf{B}} \mathbf{\Xi} \mathbf{P}_{\mathbf{1}_K}^\perp. \quad (13)$$

Given the definition of \mathbf{F} and \mathbf{G} , one knows that both of them are column orthogonal, and it can be verified that $(\mathbf{F} \otimes \mathbf{F}) \mathbf{G}$ is column orthogonal accordingly. Let $\tilde{\mathbf{D}} = \mathbf{G}^T (\mathbf{F} \otimes \mathbf{F})^T (\mathbf{F} \otimes \mathbf{F}) \mathbf{G} \in \mathbb{R}^{(2(M_1 M_2 + M_2) - 1) \times (2(M_1 M_2 + M_2) - 1)}$, then $\tilde{\mathbf{D}}$ is a diagonal matrix.

From (13), one observes that the information of the desired signals, i.e., DOAs, lie in the lower dimensional space spanned by $\tilde{\mathbf{B}}$. Thus, one can reduce the problem size by performing the following linear processing

$$\begin{aligned} \mathbf{Z} &= \tilde{\mathbf{D}}^{-\frac{1}{2}} \mathbf{G}^T (\mathbf{F} \otimes \mathbf{F})^T \mathbf{Y} \mathbf{P}_{\mathbf{1}_K}^\perp \\ &= \tilde{\mathbf{D}}^{-\frac{1}{2}} \mathbf{G}^T (\mathbf{F} \otimes \mathbf{F})^T (\mathbf{F} \otimes \mathbf{F}) \mathbf{G} \tilde{\mathbf{B}} \mathbf{\Xi} \mathbf{P}_{\mathbf{1}_K}^\perp \\ &= \tilde{\mathbf{D}}^{\frac{1}{2}} \tilde{\mathbf{B}} \mathbf{\Xi} \mathbf{P}_{\mathbf{1}_K}^\perp. \end{aligned} \quad (14)$$

From (14), it can be seen that the dimension-reduced data \mathbf{Z} are equivalent to the pseudo observations from a $2(M_1 M_2 + M_2) - 1$ -element ULA with front-end gains $\tilde{\mathbf{D}}^{\frac{1}{2}}$.

The covariance matrix \mathbf{R} of the newly constructed pseudo snapshots \mathbf{Z} is then given by

$$\mathbf{R} = E[(\mathbf{Z} - \bar{\mathbf{Z}})(\mathbf{Z} - \bar{\mathbf{Z}})^H] = (\tilde{\mathbf{D}}^{\frac{1}{2}} \tilde{\mathbf{B}}) \mathbf{R}_s (\tilde{\mathbf{D}}^{\frac{1}{2}} \tilde{\mathbf{B}})^H \quad (15)$$

where $\bar{\mathbf{Z}}$ is the mean of pseudo observations along each row of \mathbf{Z} and $\mathbf{R}_s = E[(\mathbf{\Xi} \mathbf{P}_{\mathbf{1}_K}^\perp - E[\mathbf{\Xi} \mathbf{P}_{\mathbf{1}_K}^\perp])(\mathbf{\Xi} \mathbf{P}_{\mathbf{1}_K}^\perp - E[\mathbf{\Xi} \mathbf{P}_{\mathbf{1}_K}^\perp])^H] = E[\mathbf{\Xi} \mathbf{P}_{\mathbf{1}_K}^\perp \mathbf{\Xi}^H] - E[\mathbf{\Xi} \mathbf{P}_{\mathbf{1}_K}^\perp] \cdot E[\mathbf{P}_{\mathbf{1}_K}^\perp \mathbf{\Xi}^H]$.

When $2(M_1 M_2 + M_2) - 1 \geq N$, the eigen-decomposition of \mathbf{R} can be expressed as

$$\mathbf{R} = [\mathbf{U}_s \quad \mathbf{U}_n] \begin{bmatrix} \mathbf{\Sigma}_s & \mathbf{0} \\ \mathbf{0} & \mathbf{0} \end{bmatrix} \begin{bmatrix} \mathbf{U}_s^H \\ \mathbf{U}_n^H \end{bmatrix} \quad (16)$$

where $\mathbf{U}_s \in \mathbb{C}^{(2(M_1 M_2 + M_2) - 1) \times N}$ is the eigenvector matrix associated with the N largest eigenvalues which are contained in the diagonal matrix $\mathbf{\Sigma}_s \in \mathbb{R}^{N \times N}$, $\mathbf{U}_n \in \mathbb{C}^{(2(M_1 M_2 + M_2) - 1) \times (2(M_1 M_2 + M_2) - 1 - N)}$ is the eigenvector matrix associated with the remaining eigenvalues which are all zero. The signal subspace is spanned by the columns of \mathbf{U}_s , while the noise subspace is spanned by the columns of \mathbf{U}_n .

Since both \mathbf{U}_s and $\tilde{\mathbf{D}}^{\frac{1}{2}} \tilde{\mathbf{B}}$ span the same signal subspace, there is a linear transformation between them as

$$\mathbf{U}_s = \tilde{\mathbf{D}}^{\frac{1}{2}} \tilde{\mathbf{B}} \mathbf{P} \quad (17)$$

where $\mathbf{P} \in \mathbb{C}^{N \times N}$ is a nonsingular matrix.

It is noted that the $(2(M_1M_2 + M_2) - 1) \times N$ matrix \mathbf{U}_s can be sparsely represented in the spatial domain over the entire angular grid as

$$\mathbf{U}_s = \tilde{\mathbf{D}}^{\frac{1}{2}} \tilde{\mathbf{B}}(\boldsymbol{\Theta}) \tilde{\mathbf{P}} \quad (18)$$

where $\tilde{\mathbf{B}}(\boldsymbol{\Theta})$, an over-complete dictionary, is defined as a collection of steering vectors $\tilde{\mathbf{b}}$ over the entire possible grids with $\boldsymbol{\Theta} = \{\tilde{\theta}_1, \dots, \tilde{\theta}_G\}$. We assume that the true DOAs are exactly on the sampling grid $\boldsymbol{\Theta}$ and $G \gg 2(M_1M_2 + M_2) - 1$.

It is important to note that the angular positions of the signal arrivals θ_i , $i = 1, \dots, N$, are indicated by the nonzero rows in matrix $\tilde{\mathbf{P}} = [\tilde{\mathbf{p}}_1, \dots, \tilde{\mathbf{p}}_N]$, whose values describe the corresponding coefficients associated with \mathbf{P} . Then, by introducing a vector $\mathbf{p}^0 = [p_1^0, p_2^0, \dots, p_G^0]^T$ with the g th entry p_g^0 equal to the ℓ_2 -norm of the g -th row of $\tilde{\mathbf{P}}$, i.e., $p_g^0 = \|\tilde{\mathbf{P}}(g, :)\|_2 = (\sum_{m=1}^G \tilde{p}_{g,m}^2)^{\frac{1}{2}}$ where $\tilde{p}_{g,m}$ is the m th entry of the g th row in $\tilde{\mathbf{P}}$. Generally, the non-zero entries of $\tilde{\mathbf{p}}_n$ take different values with respect to the different rows of matrix \mathbf{P} but share the same positions because they correspond to the DOAs of the same N signals. Therefore, $\tilde{\mathbf{p}}_n$ exhibits a group sparsity which can be coherently described by \mathbf{p}^0 with the same sparse structure and hence, seeking a sufficiently sparse \mathbf{p}^0 will make $\{\tilde{\mathbf{p}}_n\}_{n=1}^N$ consistently fit the eigenvectors in \mathbf{U}_s as sparsely as possible in a manner such that all the entries in a row of $\tilde{\mathbf{P}}$ tend to be zero or nonzero simultaneously, allowing the DOA estimation of quasi-stationary signals to be solved by detecting the locations of nonzero entries of \mathbf{p}^0 .

Theoretically, one should choose the ℓ_0 -norm as an ideal measure of sparsity. However, the ℓ_0 -norm minimisation problem is nonconvex, NP-hard, and mathematically intractable. Following [19,21–24] and considering the effect of finite snapshots, one can relax this to a simpler ℓ_1 -norm constrained optimisation problem, that is,

$$\min_{\mathbf{p}^0} \|\mathbf{p}^0\|_1, \quad \text{s.t.} \quad \left\| \mathbf{U}_s - \tilde{\mathbf{D}}^{\frac{1}{2}} \tilde{\mathbf{B}}(\boldsymbol{\Theta}) \tilde{\mathbf{P}} \right\|_F \leq \alpha \quad (19)$$

where α is the threshold parameter which determines the upper bound of the fitting error. It is known that large coefficients in \mathbf{p}^0 are penalised more heavily than small ones in the above optimisation problem. Thus, the exact signal recovery may not be obtained. As pointed out in [20], a reweighted ℓ_1 -norm penalty, in a form of $\|\mathbf{W}\mathbf{p}^0\|_1$ where \mathbf{W} is a diagonal matrix containing weights, can more closely resemble the ℓ_0 -norm and further enforce the sparsity, and we present a reweighted ℓ_1 -norm penalty for MMV problem here. Partitioning the over-complete dictionary $\tilde{\mathbf{B}}(\boldsymbol{\Theta})$ into two parts along the columns, without loss of generality, one, denoted as $\tilde{\mathbf{B}}_1$, is assumed to contain the N steering vectors of the true DOAs, and the other, denoted as $\tilde{\mathbf{B}}_2$, consists of the remaining steering vectors corresponding to the zero rows in the recovered matrix $\tilde{\mathbf{P}}$, giving rise to $\tilde{\mathbf{D}}^{\frac{1}{2}} \tilde{\mathbf{B}}(\boldsymbol{\Theta}) = \tilde{\mathbf{D}}^{\frac{1}{2}} [\tilde{\mathbf{B}}_1, \tilde{\mathbf{B}}_2]$. Then, inspired by the MUSIC spatial spectrum, we form the following weights

$$w_i^{(1)} = \left\| \mathbf{U}_s^H \tilde{\mathbf{D}}^{\frac{1}{2}} \tilde{\mathbf{b}}(\theta_i) \right\|_2, \quad i = 1, 2, \dots, G \quad (20)$$

and $\mathbf{w}^{(1)} = [w_1^{(1)}, \dots, w_G^{(1)}] / \max\{w_1^{(1)}, \dots, w_G^{(1)}\} = [\mathbf{w}_1, \mathbf{w}_2] / \max\{w_1^{(1)}, \dots, w_G^{(1)}\}$. As only $\tilde{\mathbf{B}}_1$ is the array manifold of the true DOAs, the weights in $\mathbf{w}_1 / \max\{w_1^{(1)}, \dots, w_G^{(1)}\}$ should be smaller than those in $\mathbf{w}_2 / \max\{w_1^{(1)}, \dots, w_G^{(1)}\}$. In particular, $\mathbf{w}_1 / \max\{w_1^{(1)}, \dots, w_G^{(1)}\} \rightarrow \mathbf{0}$ when the number of frames $K \rightarrow \infty$. Then, following the same technique in [20], one can update the

weights as

$$w_i^{(l+1)} = \frac{1}{p_i^{0(l)} + \varepsilon} \quad (21)$$

where $l \in \mathbb{Z}^+$ is the iteration count and the parameter $\varepsilon > 0$ is introduced to provide stability and to ensure that a zero-valued component in $\mathbf{p}^{0(l)}$ does not strictly prohibit a nonzero estimate at the next step. As suggested by [20], an empirical value for ε equal to 10% of the standard deviation of the nonzero coefficients of \mathbf{p}^0 is a good choice.

If the weighting matrix is defined as $\mathbf{W}^{(l)} \triangleq \text{diag}\{\mathbf{w}^{(l)}\}$, then it can more democratically penalise nonzero entries in the sparse vector \mathbf{p}^0 , that is, large weights punish the entries which are more likely to be zeros, whereas small weights preserve the large entries. By this means, the introduced $\mathbf{W}^{(l)}$ can enhance the sparse solution, and improve the accuracy of DOA estimation.

To better suppress the error, one can enforce another weighting matrix \mathbf{V} on \mathbf{U}_s , and the above reweighted ℓ_1 -norm minimisation problem turns out to be

$$\min_{\mathbf{p}^0} \|\mathbf{W}^{(l)} \mathbf{p}^0\|_1, \quad \text{s.t.} \quad \left\| \mathbf{U}_s \mathbf{V} - \tilde{\mathbf{D}}^{\frac{1}{2}} \tilde{\mathbf{B}}(\boldsymbol{\Theta}) \tilde{\mathbf{P}} \right\|_F^2 \leq \alpha. \quad (22)$$

Referring to [30], the optimal weighting matrix which gives the lowest asymptotical variance can be obtained by $\mathbf{V} = (\boldsymbol{\Sigma}_s - \sigma_n^2 \mathbf{I}_N)^2 \boldsymbol{\Sigma}_s^{-1}$ where σ_n^2 is the noise power. Ideally, σ_n^2 should be zero as shown in (15), but this is not the case in practice due to a limited number of snapshots, so it is not negligible. For this reason, σ_n^2 can be estimated as the mean of the $2(M_1M_2 + M_2) - 1 - N$ smallest eigenvalues in (15).

The sparsity-inducing solution of (22) is highly sensitive to α as this parameter determines the error tolerance, and a poor choice may lead to a non-sparse solution or largely biased estimates. Therefore, an appropriate selection of α is required to guarantee robust sparse recovery, which will be specified in the sequel.

Referring to [30], if $\tilde{\mathbf{P}}$ is exactly reconstructed, then $\frac{2K}{\sigma_n^2} \left\| \mathbf{U}_s \mathbf{V} - \tilde{\mathbf{D}}^{\frac{1}{2}} \tilde{\mathbf{B}}(\boldsymbol{\Theta}) \tilde{\mathbf{P}} \right\|_F^2$ can be expressed as a sum of the square of $2N(2(M_1M_2 + M_2) - 1 - N)$ DOFs variables that are asymptotically independent and $\mathcal{N}(0, 1)$ normal distributed, which directly results in

$$\frac{2K}{\sigma_n^2} \left\| \mathbf{U}_s \mathbf{V} - \tilde{\mathbf{D}}^{\frac{1}{2}} \tilde{\mathbf{B}}(\boldsymbol{\Theta}) \tilde{\mathbf{P}} \right\|_F^2 \sim \text{As}\chi^2(2N(2(M_1M_2 + M_2) - 1 - N)) \quad (23)$$

where $\text{As}\chi^2(2N(2(M_1M_2 + M_2) - 1 - N))$ represents the asymptotic chi-square distribution with $2N(2(M_1M_2 + M_2) - 1 - N)$ DOFs. We introduce the parameter β such that the inequality $\frac{2K}{\sigma_n^2} \left\| \mathbf{U}_s \mathbf{V} - \tilde{\mathbf{D}}^{\frac{1}{2}} \tilde{\mathbf{B}}(\boldsymbol{\Theta}) \tilde{\mathbf{P}} \right\|_F^2 \leq \beta$ is satisfied with a high probability \tilde{p} , that is,

$$\Pr\{\chi_{2N(2(M_1M_2 + M_2) - 1 - N)}^2 \leq \beta\} = \tilde{p}, \quad \beta = \chi_{2N(2(M_1M_2 + M_2) - 1 - N)}^2. \quad (24)$$

Combining the above derivation and analysis, we arrive at a statistically robust and more tractable formula for DOA estimation as follows

$$\min_{\mathbf{p}^0} \|\mathbf{W}^{(l)} \mathbf{p}^0\|_1, \quad \text{s.t.} \quad \left\| \mathbf{U}_s \mathbf{V} - \tilde{\mathbf{D}}^{\frac{1}{2}} \tilde{\mathbf{B}}(\boldsymbol{\Theta}) \tilde{\mathbf{P}} \right\|_F \leq \sqrt{\frac{\sigma_n^2}{2K} \beta}. \quad (25)$$

Obviously, problem (25) is a second-order cone programming problem and can be efficiently solved by an off-the-shelf optimisation solver such as SeDuMi [31].

In array signal processing, the incident signal can be regarded as narrowband if the maximum time delay of incident signal, τ_{\max} , impinging between the array elements is much smaller than $\frac{1}{B}$,

where $\tau_{\max} B < \frac{1}{10}$ is considered to be sufficient. However, in many other applications, such as acoustic and speech signal processing, the aforementioned condition is not satisfied, such signals are considered to be wideband, and corresponding processing methods become indispensable accordingly.

3.2. Extension to wideband signals

For wideband processing, the signal at each channel after time-sampling is partitioned into P (possibly overlapping) segments, where for each segment, N_{STFT} frequency subbands are computed by the short-time Fourier transform (STFT) and obtain $\tilde{\mathbf{x}}(f_q, t) = [\tilde{x}_1(f_q, t), \tilde{x}_2(f_q, t), \dots, \tilde{x}_M(f_q, t)]^T$ with

$$\tilde{x}_1(f_q, t) = \sum_{u=0}^{N_{\text{STFT}}-1} x(t+u) e^{-2\pi f_q u} \quad (26)$$

where N_{STFT} is the STFT window length and $f_q \in [-\frac{1}{2}, \frac{1}{2}]$ is the normalised frequency. The assumption of frequency diversity leveraged in this paper is that all signals incident from different directions share the same spectral band.

If $\tilde{\mathbf{s}}(f_q, t)$ and $\tilde{\mathbf{n}}(f_q, t)$ are defined as the STFTs of the impinging signal vector $\mathbf{s}(t)$ and the noise vector $\mathbf{n}(t)$ at the frequency bin f_q , respectively, then the array output in the frequency domain is given by

$$\tilde{\mathbf{x}}(f_q, t) \approx \mathbf{A}(f_q) \tilde{\mathbf{s}}(f_q, t) + \tilde{\mathbf{n}}(f_q, t) \quad (27)$$

where $\mathbf{A}(f_q) = [\mathbf{a}(f_q, \theta_1), \mathbf{a}(f_q, \theta_2), \dots, \mathbf{a}(f_q, \theta_N)]$ with $\mathbf{a}(f_q, \theta_i) = [1, e^{j\frac{2\pi p_2}{cT_s} f_q \sin \theta_i}, \dots, e^{j\frac{2\pi p_M}{cT_s} f_q \sin \theta_i}]^T$ being the steering vector of the 2-level nested array assuming wideband signals, c is the signal propagation speed, and T_s is the sampling period. It should be noted that, for each fixed frequency bin, the received data can be considered to fit in the narrowband signal model.

Let $\mathcal{B} \subset [0, \frac{1}{2}]$ and denote $\mathcal{B}_d = \{f_q = \frac{q}{N_{\text{STFT}}} | q = 0, 1, \dots, \frac{N_{\text{STFT}}}{2}, f \in \mathcal{B}\}$ to be a discrete version of \mathcal{B} . For each frequency component f_q , one can obtain $\mathbf{U}_{s,q}$ from (27) following the same procedures (4)–(16).

Under the sparse representation framework introduced in (18), all $\frac{N_{\text{STFT}}}{2} + 1$ eigenvector matrices $\{\mathbf{U}_{s,q}\}_{q=0}^{\frac{N_{\text{STFT}}}{2}}$ can be expressed as a unified sparse model

$$\bar{\mathbf{U}}_s = \Phi \bar{\mathbf{P}} \quad (28)$$

where $\bar{\mathbf{U}}_s = [\mathbf{U}_{s,0}^T, \dots, \mathbf{U}_{s,\frac{N_{\text{STFT}}}{2}}^T]^T$, $\Phi = (\mathbf{I} \otimes \bar{\mathbf{D}}^{\frac{1}{2}}) \text{blkdiag}\{\bar{\mathbf{B}}_0(\boldsymbol{\theta}), \dots, \bar{\mathbf{B}}_{\frac{N_{\text{STFT}}}{2}}(\boldsymbol{\theta})\}$, and $\bar{\mathbf{P}} = [\bar{\mathbf{P}}_0^T, \dots, \bar{\mathbf{P}}_{\frac{N_{\text{STFT}}}{2}}^T]^T$, with $\bar{\mathbf{B}}_q(\boldsymbol{\theta})$ and $\bar{\mathbf{P}}_q$ being the over-complete dictionary and nonsingular matrix corresponding to the frequency f_q , respectively.² Obviously, $\{\bar{\mathbf{P}}_q\}_{q=0}^{\frac{N_{\text{STFT}}}{2}}$ share the same sparse supports (i.e., nonzero coefficients) and, hence, $\bar{\mathbf{P}}^0 \triangleq [\bar{\mathbf{P}}_0, \dots, \bar{\mathbf{P}}_{\frac{N_{\text{STFT}}}{2}}]$ is a joint row N -sparse

matrix. That is, the sparsity of $\bar{\mathbf{P}}^0$ (or $\bar{\mathbf{P}}$) is only valid in spatial domain instead of the frequency domain. As a result, DOA estimation of wideband quasi-stationary signals can be cast as the following sparse reconstruction problem

$$\min_{\bar{\mathbf{P}}^0} \|\bar{\mathbf{W}}^{(l)} \bar{\mathbf{P}}^0\|_1, \quad \text{s.t.} \quad \|\bar{\mathbf{U}}_s \bar{\mathbf{V}} - \Phi \bar{\mathbf{P}}\|_F \leq \sqrt{\beta} \quad (29)$$

² The matrices or scalars with a subscript q , $q = 0, \dots, \frac{N_{\text{STFT}}}{2}$, denote those previously defined in the narrowband signal case but vary with the frequency f_q , so the interpretations of this kind of matrices or scalars will be omitted hereafter for the sake of succinctness.

where $\bar{\mathbf{W}}^{(l)} = \text{blkdiag}\{\mathbf{W}_0^{(l)}, \dots, \mathbf{W}_{\frac{N_{\text{STFT}}}{2}}^{(l)}\}$, $\bar{\mathbf{P}}^0 = [\bar{p}_1^0, \bar{p}_2^0, \dots, \bar{p}_C^0]^T$ with the g th entry \bar{p}_g^0 equal to the ℓ_2 -norm of the g th row of $\bar{\mathbf{P}}^0$, i.e., $\bar{p}_g^0 = \|\bar{\mathbf{P}}^0(g, :)\|_2 = \left(\sum_{m=1}^{G(\frac{N_{\text{STFT}}}{2}+1)} \bar{p}_{g,m}^2\right)^{\frac{1}{2}}$ where $\bar{p}_{g,m}$ is

the m th entry of the g th row in $\bar{\mathbf{P}}^0$, and $\bar{\beta} = \frac{\beta}{2K} \sum_{q=0}^{\frac{N_{\text{STFT}}}{2}} \sigma_{n,q}^2$. As $\bar{\mathbf{P}}^0$ exhibits a group sparsity across the $\frac{N_{\text{STFT}}}{2} + 1$ frequencies, the DOA estimation problem can be solved in the context of group sparse reconstruction.

It is known that the estimation resolution will be improved with by increasing the size of the array aperture. Normally, half a wavelength at a given frequency is the optimal choice for the inter-element spacing of a narrowband ULA. However, determining the inter-element spacing becomes more challenging for wideband signals since (a) the DOA estimation resolution is not optimal for other frequencies if the inter-element spacing is half a wavelength at the highest frequency component, which is conservative and inefficient; and (b) spatial aliasing may occur in signal estimation with high frequencies if the inter-element spacing is chosen to be half a wavelength at an intermediate or even lower frequency, which can make the DOA estimates unreliable for most array processing methods, e.g., [32–34]. By the virtue of sparse reconstruction, spatial aliasing can be well suppressed as long as the inter-element spacing is less than half a wavelength at the lowest frequency [35–37]. This is because different frequencies have different aliasing angles, and the proposed group sparsity recovery methods will force a common sparsity on the supports across all frequencies, indicating the true DOAs of impinging signals. In other words, the sparsity-aware methods take full advantage of the frequency diversity of the wideband signals. Therefore, the proposed method allows a larger spacing than the standard nested array while keeping aliasing-free, and better estimation accuracy and resolution can be expected.

Remark 1. The algorithm in [35] performs DOA estimation of wideband signals by covariance vector sparse representation in time domain, i.e., an SMV problem in sparse reconstruction, while both the approach in [36] and SWSR apply a quite different means—transforming the wideband signals from the time domain to frequency domain and then carrying out group sparse reconstruction in the narrowband frequency bins fitting in the framework of MMV—to accomplish DOA estimation. The main difference between the latter two is that SWSR fits the reconstructed signal subspace and the weighted signal subspace that is estimated from the data and provides an explicit guidance for choosing the fitting error threshold, whereas the technique in [36] performs a fitting between the reconstructed signals and samples given, involving much higher computational complexity if the number of snapshots is large, and scant details on the selection of a regularisation parameter are offered therein. Another approach to underdetermined wideband DOA estimation [37] is to use co-prime arrays as well as the group sparsity in all subbands; the computational complexity of this technique is reduced by removing a number of redundant elements in the difference co-array while preserving satisfactory performance, however, its group sparse reconstruction is rather common and the relevant fitting error bound is not specified.

It should be noted that the proposed estimator, SWSR, can be readily applied to K -level ($K \geq 3$) nested arrays, containing M_1, M_2, \dots, M_K sensors in each level, as the main processing procedures and equations are the same as (4)–(29) except that the sizes of related matrices, such as \mathbf{F} , \mathbf{B} , \mathbf{G} , etc. have to be changed accordingly, and the DOFs in the corresponding difference co-array become $2(\sum_{i=1}^K \sum_{j=1}^K M_i M_j + M_K - 1) + 1$ [11].

3.3. Identifiability of DOA estimation

In this section, we consider the virtual array constructed by exploiting the difference co-array and quasi-stationarity, and derive the analytical expression of the maximum number of DOFs. We consider the narrowband signal condition here, but the analysis and conclusion are also valid for the wideband signal case.

It should be noted that the dimension of the virtual array manifold $\tilde{\mathbf{D}}^{\frac{1}{2}} \tilde{\mathbf{B}}$ is $2(M_1 M_2 + M_2) - 1$, which significantly enhances the DOFs of the original linear array with M physical sensors and holds great potential in allowing more signals than sensors ($N \geq M$) to be estimated, i.e., the so-called underdetermined DOA estimation [9,11]. This problem relates to the sparsity of the nonsingular matrix $\tilde{\mathbf{P}}$ since, as is shown in (18), the DOA estimation problem relies on the sparse estimation of this matrix. The following proposition provides the key result on the parameter identifiability.

Proposition 1. *If any M -element array (possibly nonlinear) is unambiguous, then the maximum number of QSS that can be resolved is $M(M-1)$. In particular, for a 2-level nested array with M_1 and M_2 sensors ($M_1 + M_2 = M$) respectively in each level, this number is $2(M_1 M_2 + M_2 - 1)$; for a ULA, this number is $2(M-1)$. By contrast, if the array structure suffers from ambiguity, then this number is 0.*

The proof of Proposition 1 is given in Appendix A. By this proposition, if $M_1 = M_2 = \frac{M}{2}$ in each level for the 2-level nested array, underdetermined DOA estimation can be carried out as $2\left(\frac{M^2}{4} + \frac{M}{2} - 1\right) \geq M$ holds for $M \geq 2$ which is always true in reality. Interestingly, the identifiability of the proposed method with respect to the ULA is coincident with that of the KR subspace approach [9] though the derivations of these two techniques are essentially different from each other.

3.4. Computational complexity

We compare the main computational load of 4-MUSIC, KR-MUSIC, and SWSR, which comes from the fourth order and second order statistical matrix construction, eigen-decomposition, and SVD. For fair comparison, we assume all three algorithms have an identical DOF and effective aperture without redundancy in matrix constructions. The major computations involved in 4-MUSIC are to form an $(2(M_1 M_2 + M_2) - 1) \times (2(M_1 M_2 + M_2) - 1)$ FOC matrix, to perform the SVD of the cumulant matrix, and a one-dimensional spectral search, which require $\mathcal{O}(9(2(M_1 M_2 + M_2) - 1)^2 L + (2(M_1 M_2 + M_2) - 1)^3 + G((2(M_1 M_2 + M_2) - 1)^2 + 1) + ((2(M_1 M_2 + M_2) - 1)^2 - N))$ flops where L is the number of snapshots. Here, a flop stands for a complex-valued floating point multiplication operation. KR-MUSIC constructs two covariance matrices, of size $M \times M$ and $(2(M_1 M_2 + M_2) - 1) \times (2(M_1 M_2 + M_2) - 1)$, performs an eigen-decomposition of the $(2(M_1 M_2 + M_2) - 1) \times (2(M_1 M_2 + M_2) - 1)$ matrix, and a one-dimensional spectral search, respectively, and it thus needs $\mathcal{O}(M^2 L + (2(M_1 M_2 + M_2) - 1)^4 K + (2(M_1 M_2 + M_2) - 1)^3 + G((2(M_1 M_2 + M_2) - 1)^2 + 1) + ((2(M_1 M_2 + M_2) - 1)^2 - N))$ flops in total. By comparison, besides the same manipulations as KR-MUSIC, SWSR builds a $G \times G$ weighting matrix and carries out sparse reconstructions. The resulting flops involved are in the order of $\mathcal{O}(M^2 L + (2(M_1 M_2 + M_2) - 1)^4 K + (2(M_1 M_2 + M_2) - 1)^3 + G((2(M_1 M_2 + M_2) - 1)^2 + 1) + ((2(M_1 M_2 + M_2) - 1)^2 - N) + N^3 G^3)$. As typically $L \gg K$ and G is relatively large, say several hundreds, SWSR has the highest computational complexity among the three algorithms, followed by 4-MUSIC and then KR-MUSIC.

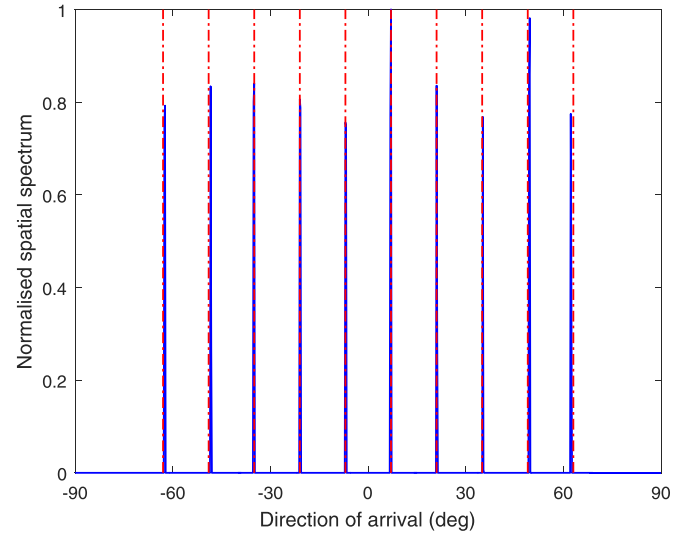


Fig. 2. Normalised spatial spectra of SWSR under the maximum identifiability. SNR = 10 dB, $L = 300$, and $K = 300$. The dashed lines in red mark the true DOA positions.

4. Simulation results and discussion

In this section, a series of numerical experiments under different conditions are conducted to examine the performance of the proposed sparsity-aware method, SWSR. Simulations are carried out for a 2-level nested array with 2 elements in each level, and a total of 4 sensors are deployed at $\{0, d_l, 2d_l, 5d_l\}$ where $d_l = \frac{\lambda}{2}$. Throughout this section, the spatial noise complies with a zero-mean complex Gaussian distribution which is not necessarily white. The input signal-to-noise ratio (SNR) is defined as $10 \log_{10} \left(\frac{\frac{1}{T} \sum_{t=0}^{T-1} E\{\|\mathbf{A}\mathbf{s}(t)\|_2^2\}}{E\{\|\mathbf{n}(t)\|_2^2\}} \right)$ where $T = LK$ is the total number of snapshots. The probability \tilde{p} for β in the proposed algorithm is set at 0.999.

4.1. Spatial spectra of SWSR

The maximum number of resolvable signals of SWSR is $2(M_1 M_2 + M_2 - 1) = 10$. To verify this identifiability, we consider 10 incident narrowband signals uniformly distributed from -63° to 63° with uniformly white noise. It is assumed that the SNR is 10 dB, the length of each frame is $L = 300$, and the number of frames is $K = 300$. To reduce the computational complexity and improve the estimation accuracy, we first use a coarse grid in the range of $[-90^\circ, 90^\circ]$ with a step size of 1° , and then set a refined grid spacing of 0.05° around the estimated peaks.

Fig. 2 depicts the normalised spatial spectra of SWSR. The dash lines indicate the true DOAs. It can be seen that each DOA can be correctly determined even though the number of signals is larger than the number of sensors. Next, we compare the spectra obtained using SWSR with those of 4-MUSIC [38,39] and KR-MUSIC [9] with respect to the angular resolution between two closely separated signals $[-35^\circ, -30^\circ]$. In Fig. 3, we decrease the SNR and L to -5 dB and 50, respectively, and only the proposed sparsity-aware method is able to resolve the two signals, whereas both 4-MUSIC and KR-MUSIC merge the two peaks.

The bias of SWSR introduced by using the sparse representation is now examined in terms of the angular separation between two signals. Assume two equal-power uncorrelated signals arrive from $\theta = -30^\circ$ and $\theta = -30^\circ + \Delta\theta$, respectively, where $\Delta\theta$ is varied from 1° to 50° in 1° steps. The SNR is set to 6 dB. Fig. 4 indicates that the estimation bias of SWSR becomes close to zero when $\Delta\theta$ exceeds 25° .

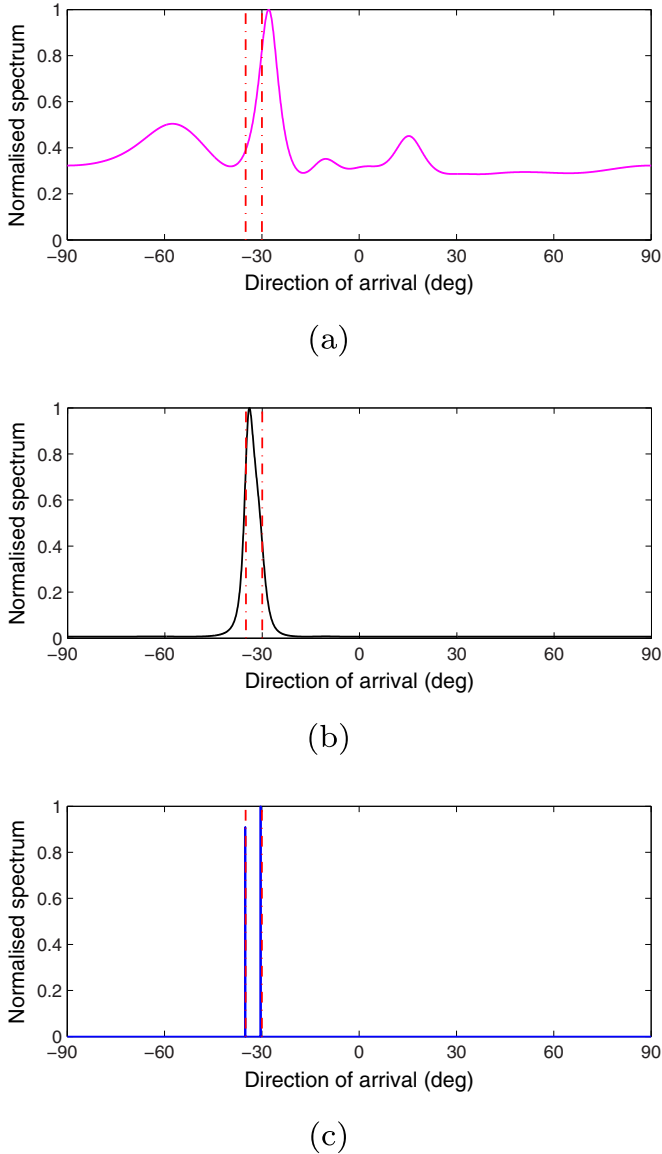


Fig. 3. Spatial spectra of (a) 4-MUSIC, (b) KR-MUSIC, and (c) SWSR for two closely separated signals. SNR = -5 dB, $L = 300$, and $K = 50$. The dashed lines in red mark the true DOA positions.

Fig. 5 shows the spatial spectra of the three algorithms with a small number of frames, say $K = 15$, fixing SNR = 5 dB and $L = 500$. Assume there are eight QSS from $[-60^\circ, -45^\circ, -30^\circ, 0^\circ, 15^\circ, 30^\circ, 45^\circ]$ impinging on the array. As it can be seen, KR-MUSIC and SWSR exhibit consistent spectral peaks with respect to the true DOAs, but the peaks of SWSR are much sharper in comparison, whereas 4-MUSIC can only identify 6 signals and has a large bias on the DOA estimates.

Next, we consider a wideband microphone array processing system and test the robustness of the algorithms to spatial aliasing occurring in the wideband signal case. Assume 5 signals from $[-65^\circ, -56^\circ, -45^\circ, 20^\circ, 45^\circ]$ with a common bandwidth of 1 kHz impinging on the array. The grid spacing is set as 1° within $[-90^\circ, 90^\circ]$. The sampling frequency is $F_s = 6.4$ kHz. The STFT window length is $N_{STFT} = 128$. The frame length and the number of frames are $L = 400$ and $K = 100$, respectively. The frequency band processed is $\mathcal{B}_d = \begin{bmatrix} 1500 & 3000 \\ 6400 & 6400 \end{bmatrix}$ corresponding to $q = 30, 31, \dots, 60$. The inter-element spacing $d_l = 8.5$ cm under a sound propagation speed of $c = 340$ m/s is equivalent to the half-wavelength of 2 kHz.

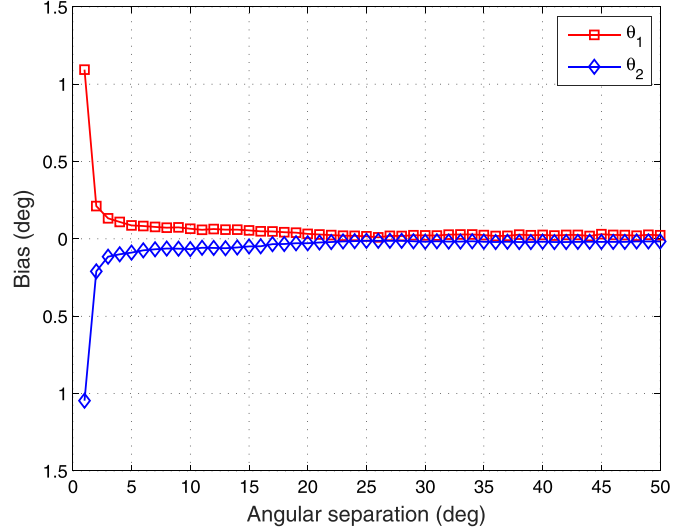


Fig. 4. Bias of SWSR versus angular separation of two sources. SNR = 6 dB, $L = 500$, and $K = 50$.

As such, spatial aliasing may occur when the analogue frequency $f_a > 2$ kHz for 4-MUSIC and KR-MUSIC, which, however, can be well suppressed by the proposed sparse recovery algorithm as long as it is less than the half-wavelength of the lowest frequency. The frequency-bearing images are plotted in Fig. 6. It can be seen that spatial aliasing appears in the KR-MUSIC when $f_a > 2$ kHz, but no aliasing is observed in the proposed estimator.

4.2. RMSE performance

In this subsection, we examine the RMSE Performance of 4-MUSIC, KR-MUSIC, and SWSR under spatially coloured noise. Such noise is assumed to be a first order spatial autoregressive process, and the (m, n) th entry of the noise covariance matrix is given by $\mathbf{R}(m, n) = \sigma_n^2 0.8^{|m-n|} e^{j\frac{\pi(m-n)}{16}}$ [40]. The accuracy of the DOA estimate is measured from 800 Monte Carlo runs in terms of the root mean square error (RMSE) which is defined as

$$\text{RMSE} = \sqrt{\frac{1}{800N} \sum_{n=1}^{800} \sum_{i=1}^N (\hat{\theta}_i^{(n)} - \theta_i)^2} \quad (30)$$

where $\hat{\theta}_i^{(n)}$ is the estimate of θ_i for the n th trial, and N is the number of QSS. Fig. 7 depicts the RMSE of the DOA estimates of three signals from $[-35^\circ, -28^\circ, 20^\circ]$. From this figure, we can see that as the SNR and the number of snapshots increase, the RMSE of DOA estimation decreases gradually for both KR-MUSIC and SWSR. The simulation results in Fig. 7(a) indicate that the proposed sparse reconstruction approach succeeded in separating the three signals at lower SNR. This superior resolution performance of sparse recovery applied in low SNR regime is natural, which has been widely shown in the literature [19,21–25]. Meanwhile, SWSR has the best estimation performance with respect to variation of SNR. The results in Fig. 7(b) indicate that SWSR requires only a small number of frames to achieve super-resolution, and the proposed sparsity-inducing method has smaller RMSE than KR-MUSIC all through. As the number of frames increases, the DOA estimation accuracy of KR-MUSIC improves dramatically and approaches SWSR with a small margin at $K = 50$ or even larger. Fig. 7(c) evaluates the respective RMSE by varying frame length L where the total signal length $T = LK$ and SNR is fixed at 9000 and 14 dB, respectively. It can be observed that KR-MUSIC is less accurate than SWSR, whereas 4-MUSIC fails to work. The best frame length for both KR-MUSIC and SWSR is about 400, and the two methods show

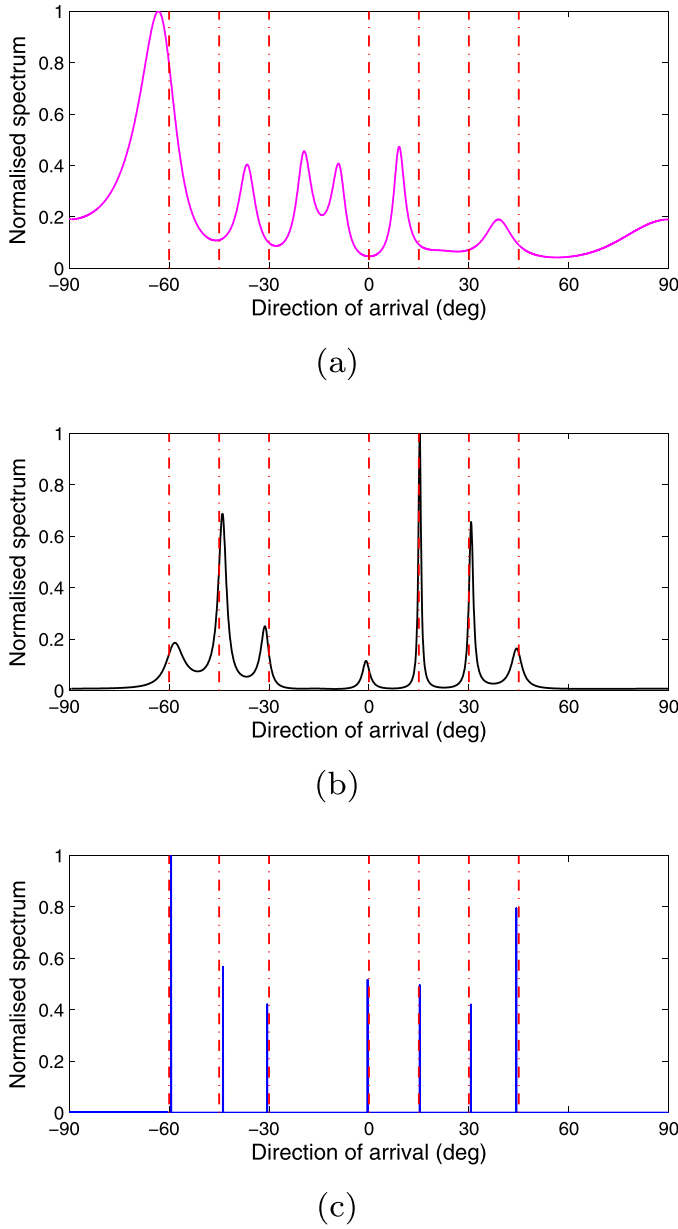


Fig. 5. Spatial spectra of (a) 4-MUSIC, (b) KR-MUSIC, and (c) SWSR with a small number of frames. SNR = 5 dB, $L = 500$, and $K = 15$. The dashed lines in red mark the true DOA positions.

mild performance degradation when L is decreased down to 100, which is due to estimation errors of the local covariances calculated from limited local snapshot size. Besides, this set of empirical results suggests that for a fixed data size RMSE performance degrades when L is large.

Next, we consider nine signals uniformly distributed from $[-56^\circ, 56^\circ]$ impinging on the array. Based on the simulation settings, the results of the RMSE versus SNR and the number of snapshots are depicted in Fig. 8. As shown in Fig. 8(a), excluding 4-MUSIC, KR-MUSIC and SWSR are able to identify all signals at moderate SNRs, but among them, KR-MUSIC clearly has a larger DOA estimation RMSE than the proposed sparsity-aware technique. The results in Fig. 8(b) demonstrate that KR-MUSIC and SWSR require only 30 frames to achieve super-resolution, and SWSR is still superior to KR-MUSIC for all K . We also note that 4-MUSIC is not able to separate all the signals in the considered scenarios even though as many as 120 frames are collected. In Fig. 8(c), we plot the RMSE

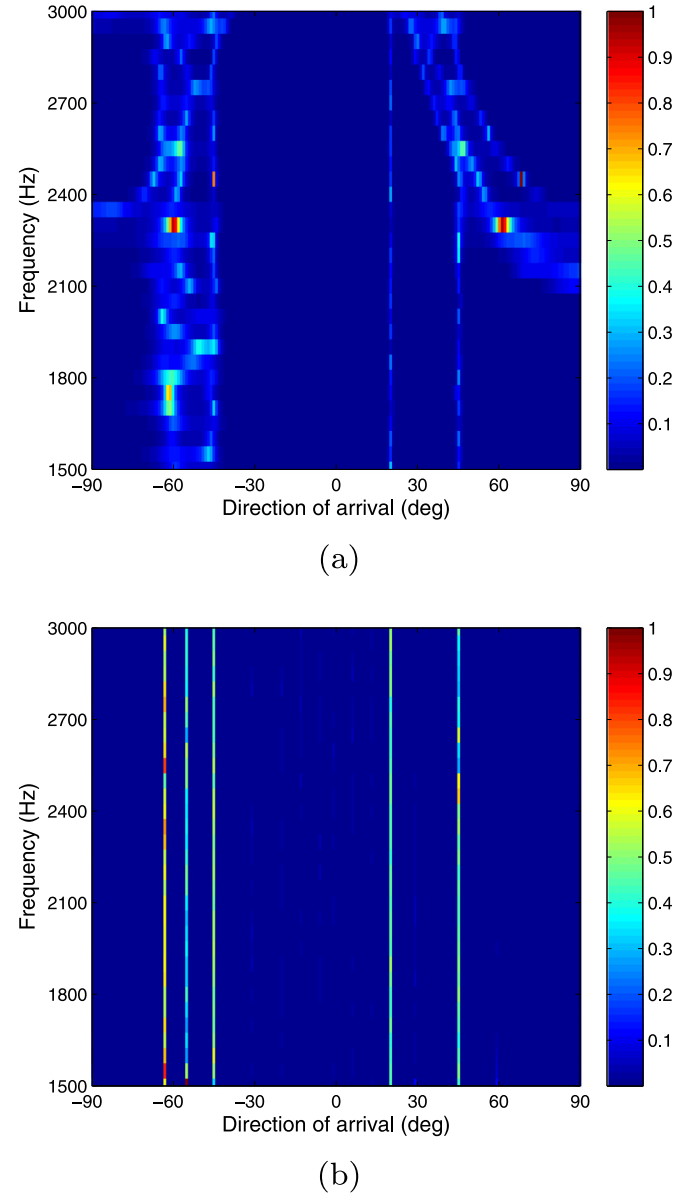
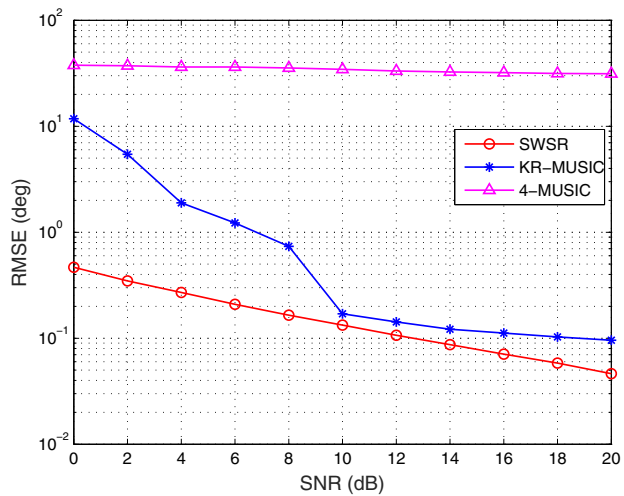


Fig. 6. Frequency-bearing images of (a) KR-MUSIC and (b) SWSR. SNR = 0 dB, $L = 400$, and $K = 100$.

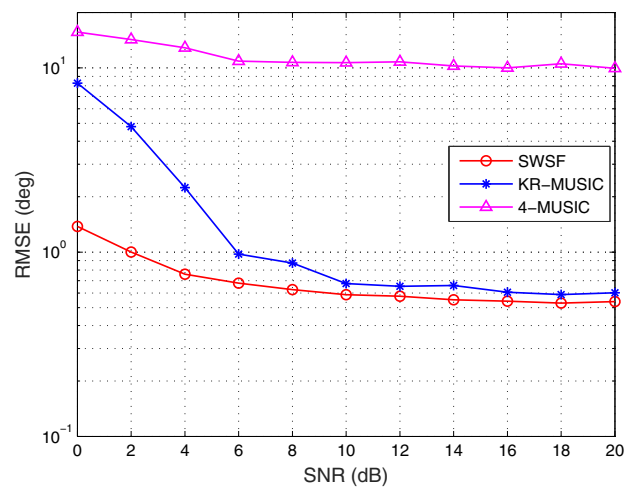
performance versus the frame length for the three methods when $T = 24000$ and SNR = 5 dB. It illustrates that the optimal frame length for both KR-MUSIC and SWSR is about 150, and SWSR is superior to KR-MUSIC and 4-MUSIC for all frame lengths.

5. Conclusion

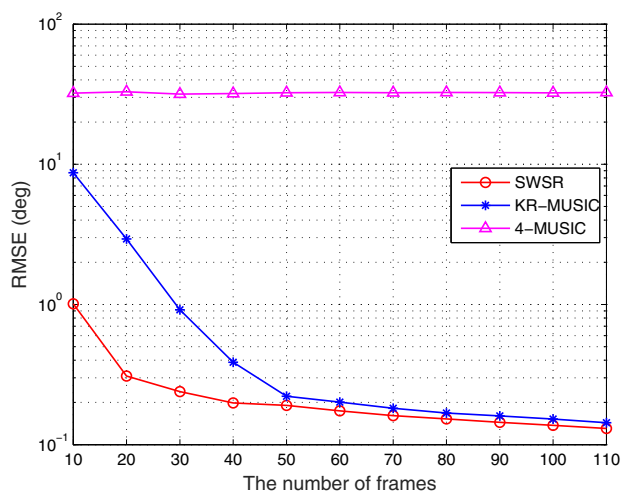
In this paper, we have applied sparse support reconstruction to DOA estimation of QSS using a nested array. For the nested array, a dimension reduction technique arises in the process of formulating the virtual array with extended effective aperture and more DOFs. A new algorithm based on sparse reconstruction was proposed to estimate DOAs utilising the difference co-array with multiple pseudo snapshots, thereby increasing the DOF from $\mathcal{O}(M)$ to $\mathcal{O}(M^2)$. As the sparsity-inducing techniques have clear advantages on estimation accuracy and resolution in adverse scenarios like low SNRs or a small number of snapshots (frames) over subspace-based algorithms, we imported the sparse reconstruction scheme to QSS. Based on the novel signal model and the statistical



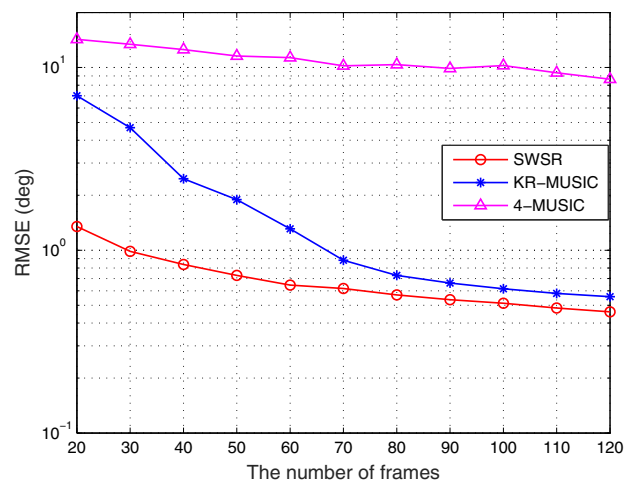
(a)



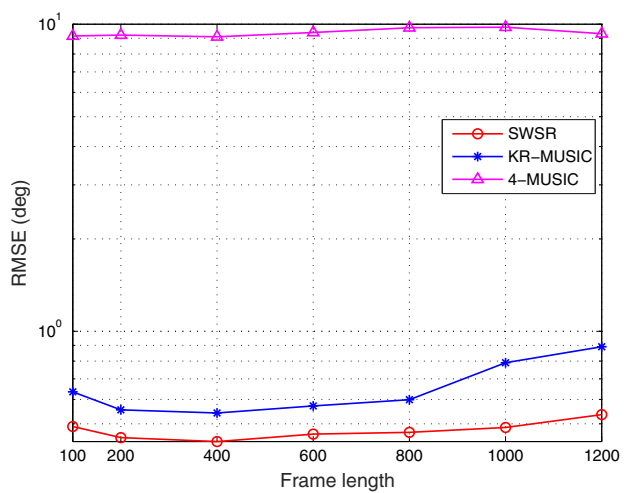
(a)



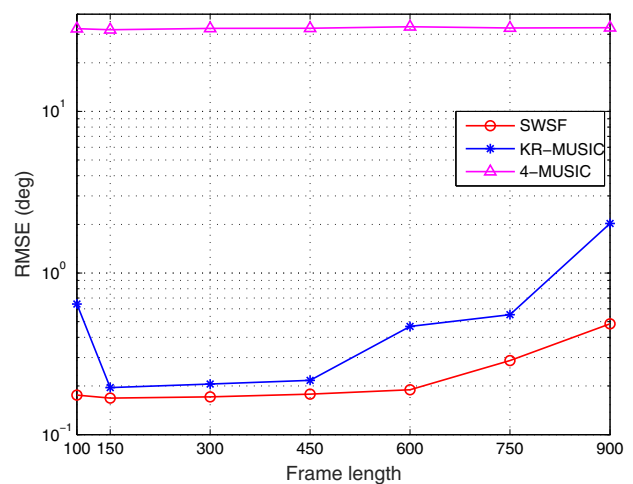
(b)



(b)



(c)



(c)

Fig. 7. RMSE of the DOA estimates in the overdetermined case versus (a) SNR when $L = 150$ and $K = 30$; (b) K when $\text{SNR} = 5$ dB and $L = 150$; (c) L when $T = 9000$ and $\text{SNR} = 5$ dB.

Fig. 8. RMSE of the DOA estimates in the underdetermined case versus (a) SNR when $L = 200$ and $K = 50$; (b) K when $\text{SNR} = 5$ dB and $L = 200$; (c) L when $T = 24000$ and $\text{SNR} = 5$ dB.

property of samples signal subspace perturbation, we cast the DOA estimation problem as a reweighted ℓ_1 -norm minimisation subject to a weighted error-constrained Frobenius norm. By numerical simulation experiments, we have verified that the proposed method has significantly enhanced adaptation than some state-of-the-art algorithms in demanding scenarios with low SNR, limited frames and spatially adjacent signals, it also obtains considerably more accurate DOA estimates. Meanwhile, the developed approach also makes good use of the nested array geometry to enhance its ability in separating more simultaneous signals than the number of physical sensors.

Appendix A. Proof of Proposition 1

Proof. First of all, we consider the generic array geometry which is formed by randomly distributed sensors. By the principle of co-array, the maximum DOFs achievable from $\tilde{\mathbf{A}} \triangleq \mathbf{A}^* \circ \mathbf{A}$ is $\text{DOF}_{\max}^{\tilde{\mathbf{A}}} = M(M-1) + 1$. Without ambiguities in array structure, we have $\text{Spark}(\tilde{\mathbf{A}}(\boldsymbol{\theta})) = M(M-1) + 2$ where $\text{Spark}(\tilde{\mathbf{A}}(\boldsymbol{\theta}))$ denotes the smallest possible integer of columns of $\tilde{\mathbf{A}}(\boldsymbol{\theta})$ that are linearly dependent. It is known that a coefficient vector $\tilde{\mathbf{p}}$ is said to be k sparse if the size of the support of $\tilde{\mathbf{p}}$ is no larger than k : $|\text{supp}(\tilde{\mathbf{p}})| \leq k$. We define the support of a collection of vectors $\tilde{\mathbf{P}} = [\tilde{\mathbf{p}}_1, \dots, \tilde{\mathbf{p}}_C]$ as the union over all the individual supports:

$$|\text{supp}(\tilde{\mathbf{P}})| := \bigcup_i \text{supp}(\tilde{\mathbf{p}}_i). \quad (\text{A.1})$$

A matrix $\tilde{\mathbf{P}}$ is called k joint sparse if $|\text{supp}(\tilde{\mathbf{P}})| \leq k$. In other words, there are at most k rows in $\tilde{\mathbf{P}}$ that contain nonzero entries.

According to Theorem 2.4 of [41], there exists a unique sparsest representation $\tilde{\mathbf{P}}$ such that $\tilde{\mathbf{U}}_s = \tilde{\mathbf{A}}(\boldsymbol{\theta})\tilde{\mathbf{P}}$ if and only if

$$\begin{aligned} |\text{supp}(\tilde{\mathbf{P}})| &< \frac{\text{Spark}(\tilde{\mathbf{A}}(\boldsymbol{\theta})) - 1 + \text{rank}(\tilde{\mathbf{U}}_s)}{2} \\ &= \frac{M(M-1) + 1 + \text{rank}(\tilde{\mathbf{U}}_s)}{2} \end{aligned} \quad (\text{A.2})$$

where $\tilde{\mathbf{U}}_s$ is the eigenvector matrix sharing the same signal subspace with $\tilde{\mathbf{A}}$. It is readily seen that $1 \leq \text{rank}(\tilde{\mathbf{U}}_s) \leq M(M-1) + 1$ provided that $K \geq M(M-1) + 2$, i.e., the number of frames of quasi-stationary signals is sufficiently large. Accordingly, we have

$$|\text{supp}(\tilde{\mathbf{P}})| < \frac{M(M-1) + 1 + M(M-1) + 1}{2} = M(M-1) + 1 \quad (\text{A.3})$$

which implies that

$$|\text{supp}(\tilde{\mathbf{P}})| \leq M(M-1). \quad (\text{A.4})$$

Therefore, the maximum resolvable signal number is $M(M-1)$.

Then, we take the 2-level nested array as an instance of special array geometries to analyse. It is easy to identify that $\text{Spark}(\tilde{\mathbf{D}}^{\frac{1}{2}}\tilde{\mathbf{B}}(\boldsymbol{\theta})) = 2(M_1M_2 + M_2)$ because $\text{DOF}_{\max}^{\tilde{\mathbf{B}}} = 2(M_1M_2 + M_2) - 1$ again from the co-array principle. From the sufficient condition (A.2), the maximum number of resolvable signals is $2(M_1M_2 + M_2 - 1)$. In a similar manner, this number for the ULA is $2(M-1)$ since the DOF of ULA manifold is $2M-1$. On the other hand, if the array structure suffers from ambiguity, then $\text{Spark}(\tilde{\mathbf{A}}(\boldsymbol{\theta})) = 2$, which directly leads to the uniqueness condition $|\text{supp}(\tilde{\mathbf{P}})| = 0$ from (A.2). This completes the proof of Proposition 1. \square

References

- [1] R.O. Schmidt, Multiple emitter location and signal parameter estimation, *IEEE Trans. Antennas Propag.* 34 (3) (1986) 276–280.
- [2] R. Roy, T. Kailath, ESPRIT—Estimation of signal parameters via rotational invariance techniques, *IEEE Trans. Acoust., Speech, Signal Process.* 37 (7) (1989) 984–995.
- [3] P. Chargé, Y. Wang, J. Saillard, A non-circular sources direction finding method using polynomial rooting, *Signal Process.* 81 (8) (2001) 1765–1770.
- [4] J. Li, P. Stoica, MIMO radar with colocated antennas, *IEEE Signal Process. Mag.* 24 (5) (2007) 106–114.
- [5] A. Moffet, Minimum-redundancy linear arrays, *IEEE Trans. Antennas Propag.* 16 (2) (1968) 172–175.
- [6] R.T. Hoctor, S.A. Kassam, The unifying role of the co-array in aperture synthesis for coherent and incoherent imaging, *Proc. IEEE* 78 (4) (1990) 735–752.
- [7] F. Asano, S. Hayamizu, T. Yamada, S. Nakamura, Speech enhancement based on subspace method, *IEEE Trans. Speech Audio Process.* 8 (5) (2000) 497–507.
- [8] L. Rankine, N. Stevenson, M. Mesbah, B. Boashash, A nonstationary model of newborn EEG, *IEEE Trans. Biomed. Eng.* 54 (1) (2007) 19–28.
- [9] W.-K. Ma, T.-H. Hsieh, C.-Y. Chi, DOA estimation of quasi-stationary signals with less sensors than sources and unknown spatial noise covariance: A Khatri-Rao subspace approach, *IEEE Trans. Signal Process.* 58 (4) (2010) 2168–2180.
- [10] M. Cao, L. Huang, C. Qian, J. Xue, H. So, Underdetermined DOA estimation of quasi-stationary signals via Khatri-Rao structure for uniform circular array, *Signal Process.* 106 (2015) 41–48.
- [11] P. Pal, P.P. Vaidyanathan, Nested arrays: a novel approach to array processing with enhanced degrees of freedom, *IEEE Trans. Signal Process.* 58 (8) (2010) 4167–4181.
- [12] S. Li, W. He, X. Yang, M. Bao, Y. Wang, Direction-of-arrival estimation of quasi-stationary signals using two-level Khatri-Rao subspace and four-level nested array, *J. Cent. South Univ.* 21 (7) (2014) 2743–2750.
- [13] C.-L. Liu, P.P. Vaidyanathan, Remarks on the spatial smoothing step in coarray MUSIC, *IEEE Signal Process. Lett.* 22 (9) (2015) 1438–1442.
- [14] P. Pal, P.P. Vaidyanathan, A grid-less approach to underdetermined direction of arrival estimation via low rank matrix denoising, *IEEE Signal Process. Lett.* 21 (6) (2014) 737–741.
- [15] E.J. Candès, T. Tao, Decoding by linear programming, *IEEE Trans. Inf. Theory* 51 (12) (2005) 4203–4215.
- [16] D.L. Donoho, M. Elad, V.N. Temlyakov, Stable recovery of sparse overcomplete representation in the presence of noise, *IEEE Trans. Inf. Theory* 52 (1) (2006) 6–18.
- [17] I.F. Gorodnitsky, B.D. Rao, Sparse signal reconstruction from limited data using FOCUSS: a re-weighted minimum norm algorithm, *IEEE Trans. Signal Process.* 45 (3) (1997) 600–616.
- [18] J.-J. Fuchs, On the application of the global matched filter to DOA estimation with uniform circular arrays, *IEEE Trans. Signal Process.* 49 (4) (2001) 702–709.
- [19] D. Malioutov, M. Çetin, A.S. Willsky, A sparse signal reconstruction perspective for source localization with sensor arrays, *IEEE Trans. Signal Process.* 53 (8) (2005) 3010–3022.
- [20] E.J. Candès, M.B. Wakin, S.P. Boyd, Enhancing sparsity by reweighted ℓ_1 minimization, *J. Fourier Anal. Appl.* 14 (5–6) (2008) 877–905.
- [21] X. Xu, X. Wei, Z. Ye, DOA estimation based on sparse signal recovery utilizing weighted ℓ_1 -norm penalty, *IEEE Signal Process. Lett.* 19 (3) (2012) 155–158.
- [22] J. Yin, T. Chen, Direction-of-arrival estimation using a sparse representation of array covariance vectors, *IEEE Trans. Signal Process.* 59 (9) (2011) 4489–4493.
- [23] N. Hu, Z. Ye, X. Xu, M. Bao, DOA estimation for sparse array via sparse signal reconstruction, *IEEE Trans. Aerosp. Electron. Syst.* 49 (2) (2013) 760–773.
- [24] J. Zheng, M. Kaveh, Sparse spatial spectral estimation: a covariance fitting algorithm, performance and regularization, *IEEE Trans. Signal Process.* 61 (11) (2013) 2767–2777.
- [25] Y. Tian, X. Sun, S. Zhao, DOA and power estimation using a sparse representation of second-order statistics vector and ℓ_0 -norm approximation, *Signal Process.* 105 (2014) 98–108.
- [26] P. Stoica, B. Prabhhu, L. Jian, SPICE: a sparse covariance-based estimation method for array processing, *IEEE Trans. Signal Process.* 59 (2) (2011) 629–638.
- [27] M.M. Hyder, K. Mahata, Direction-of-arrival estimation using a mixed $\ell_{2,0}$ norm approximation, *IEEE Trans. Signal Process.* 58 (9) (2010) 4646–4655.
- [28] Q. Shen, W. Liu, W. Cui, S. Wu, Extension of co-prime arrays based on the fourth-order difference co-array concept, *IEEE Signal Process. Lett.* 23 (5) (2016) 615–619.
- [29] M. Jansson, B. Góransson, B. Ottersten, A subspace method for direction of arrival estimation of uncorrelated emitter signals, *IEEE Trans. Signal Process.* 47 (4) (1999) 945–956.
- [30] M. Viberg, B. Ottersten, T. Kailath, Detection and estimation in sensor arrays using weighted subspace fitting, *IEEE Trans. Signal Process.* 39 (11) (1991) 2436–2449.
- [31] J.F. Sturm, Using sedumi 1.02, a MATLAB toolbox for optimization over symmetric cones, *Optim. Methods Softw.* 11 (1–4) (1999) 625–653.
- [32] G. Su, M. Morf, The signal subspace approach for multiple wideband emitter location, *IEEE Trans. Acoust., Speech, Signal Process.* 31 (6) (1983) 1502–1522.
- [33] H. Wang, M. Kaveh, Coherent signal-subspace processing for the detection and estimation of angles of arrival of multiple wide-band sources, *IEEE Trans. Acoust., Speech, Signal Process.* 33 (4) (1985) 823–831.
- [34] Y.-S. Yoon, L.M. Kaplan, J.H. McClellan, TOPS: new DOA estimator for wideband signals, *IEEE Trans. Signal Process.* 54 (6) (2006) 1977–1989.

- [35] Z. Liu, Z. Huang, Y. Zhou, Direction-of-arrival estimation of wideband signals via covariance matrix sparse representation, *IEEE Trans. Signal Process.* 59 (9) (2011) 4256–4270.
- [36] Z. Tang, G. Blacqui re, G. Leus, Aliasing-free wideband beamforming using sparse signal representation, *IEEE Trans. Signal Process.* 59 (7) (2011) 3464–3469.
- [37] Q. Shen, W. Liu, W. Cui, S. Wu, Y.D. Zhang, M.G. Amin, Low-complexity direction-of-arrival estimation based on wideband coprime arrays, *IEEE/ACM Trans. Audio, Speech, Lang. Process.* 23 (9) (2015) 1445–1456.
- [38] B. Porat, B. Friedlander, Direction finding algorithms based on high-order statistics, *IEEE Trans. Signal Process.* 39 (9) (1991) 2016–2024.
- [39] M.C. Dogan, J.M. Mendel, Applications of cumulants to array processing part I: aperture extension and array calibration, *IEEE Trans. Signal Process.* 43 (5) (1995) 1200–1216.
- [40] M. Viberg, P. Stoica, B. Ottersten, Maximum likelihood array processing in spatially correlated noise fields using parameterized signals, *IEEE Trans. Signal Process.* 45 (4) (1997) 996–1004.
- [41] J. Chen, X. Huo, Theoretical results on sparse representations of multiple-measurement vectors, *IEEE Trans. Signal Process.* 54 (12) (2006) 4634–4643.